Chemistry–A European Journal
Research Article
doi.org/10.1002/chem.202300845
Chemistry Europe
European Chemical Societies Publishing
www.chemeurj.org

Massively Parallel Double-Selection Workflow for the Evolution of Molecular Switches Based on Surface-Display in *Escherichia coli*

Louis Givelet,[a] Alexandra Bienau,[a] and Friedrich C. Simmel*[a]

Abstract: Microbial surface display of proteins is a versatile method for a wide range of biotechnological applications. Herein, the use of a surface display system in *E. coli* for the evolution of a riboswitch from an RNA aptamer is presented. To this end, a streptavidin-binding peptide (SBP) is displayed at the bacterial surface, which can be used for massively parallel selection using a magnetic separation system. Coupling gene expression from a riboswitch library to the display of SBP hence allows selection of library members that express strongly in the presence of a ligand. As excessive SBP expression leads to bacterial growth inhibition, it can be used to negatively select against leaky riboswitches expressing in the absence of ligand. Based on this principle, we devise a double selection workflow that enables quick selection of functional riboswitches with a comparatively low screening workload. The efficiency of our protocol by re-discovering a previously isolated theophylline riboswitch from a library was demonstrated, as well as a new riboswitch that is similar in performance, but slightly more responsive at low theophylline concentrations. Our workflow is massively parallel and can be applied to the screening or pre-screening of large molecular libraries.

Introduction

Surface display technology has undergone significant development and diversification in the past four decades. While the first surface displayed heterologous protein expression was achieved in bacteriophages,[1] the technology was rapidly generalized to cell surface display with gram negative bacteria,[2] gram positive bacteria,[3] yeast[4] and mammalian cells.[5] In cell surface display systems, the target is first expressed within the cytoplasm, but then exported and subsequently presented on the cell surface, thus exposing it to the extracellular medium. The complexity of the surface displayed molecules gradually increased over the years, starting first from short peptides to active enzymes,[6] large proteins[7] and even to multiple enzymes displayed together.[8] Based on these achievements, surface display found a wide range of applications in vaccine development,[9] in whole-cell catalysts,[6a,b,10] biosensors,[11] and library screening. Screening has been performed with peptides,[12] nanobodies[13] or enzyme[14] libraries. Importantly, surface display technology allows to screen the displayed library variants through an assay, while retaining the genetic material associated with them in the cells, therefore maintaining the critical link between phenotype and genotype.

Among the various screening systems in use, *Escherichia coli* is particularly suitable for high-throughput screening of large molecular libraries ($>10^7$ library members). Next to established molecular cloning procedures, *E. coli* offers good plasmid stability, fast growth, high cell density and, importantly, a high transformation efficiency, thus enabling the manipulation and maintenance of large libraries in vivo. Moreover, *E. coli* can be submitted to selection by fluorescence activated cell sorting (FACS), making library evaluation relatively easy. While these intrinsic features make *E.* coli generally useful for library screening, cell surface display faces the challenge that any material to be displayed on the surface of this gram-negative bacterium must cross two biological membranes (the periplasmic and the outer membrane). This issue has been successfully tackled in a wide range of studies,[13,15] which effectively rendered *E. coli* a suitable host also for many surface-display applications.

In the present work we will focus on the use of a surface display technique for the selection of riboswitches, which are an interesting and challenging class of molecular targets for directed evolution through library screening. Discovered in 2002,[16] riboswitches are RNA sequences found in bacteria, archaea, fungi and plants[17] acting as regulatory devices through the binding of a specific substrate. They are comprised of two domains: a sensing domain (an RNA aptamer) responsible for substrate binding, and an expression platform controlling the expression of the gene located downstream of the riboswitch (e.g., via the accessibility of a ribosome binding site). Binding of a ligand to the aptamer domain triggers a

[a] *L. Givelet, A. Bienau, Prof. Dr. F. C. Simmel*
Technical University Munich
School of Natural Sciences
Department of Bioscience
Chair of Physics of Synthetic Biological Systems
Am Coulombwall 4a, 85748 Garching (Germany)
E-mail: simmel@tum.de

Supporting information for this article is available on the WWW under https://doi.org/10.1002/chem.202300845

conformational change in the expression platform, leading either to gene repression or activation.[18] In order to achieve a high ON/OFF ratio of expression levels, the sensing domain must have a very good affinity for the substrate and must be capable of a conformational change upon ligand binding. Such a change has to be propagated to the expression platform and result in a significant effect on gene expression efficiency. Due to their mutual influence on each other, optimization of these requirements is a complex task, and even when the sensing domain is already known, turning an aptamer into a functional riboswitch is not straightforward.[19] Directed evolution of a switch has to meet two objectives: selected sequences have to result in low expression levels when the switch is supposed to be in the OFF state, but display a high expression when the switch is expected to be in the ON state (in the absence or presence of ligand, depending on which kind of switch is evolved).

Despite these challenges, riboswitches have the advantage that the main parameters to evolve (ON or OFF expression rates) can be directly connected to the expression of any desired gene product, which allows to turn cells into functionalized compartments for directed evolution. Using this advantage, inventive ways of selection have already been devised, for instance, selection based on antibiotic resistance[20] or chemotaxis.[21] Such systems can achieve a very high throughput given that the selection happens in bulk and therefore is not dependent on sampling speed as in other high-throughput approaches (such as FACS or colony picking robots). Therefore, the time required for screening of a large library is not linearly dependent on its size.

Here we present the application of a surface display system as a selection system to perform in vivo directed evolution on a riboswitch expression platform library. Optimal protocols and parameters were determined experimentally with mock selections and then successfully applied to develop riboswitches for a known molecular target, theophylline. We envision that our system can be utilized for massively parallel pre-selection to be applied to a library prior to the use of other high-throughput methods, which reduces the workload when screening variants individually, and thus speeds up the overall selection procedure.

Results and Discussion

Magnetic separation by surface display of a streptavidin-binding peptide

In order to develop an in vivo high-throughput selection system, we engineered *E. coli* cells to be able to bind to a ligand molecule present in the extra-cellular medium via surface display of the corresponding binder. To this end, we decided to employ a previously developed system,[22] which displays the Streptavidin-Binding-Peptide (SBP) on the *E. coli* cell surface with the help of an Lpp-OmpA construct. Even though it is only 38 amino acids long, SBP has a high affinity for streptavidin[23] ($K_D = 2.4$ nM), which is a major advantage for use in surface display, for which the size of the passenger protein size is usually a critical factor. The Lpp-OmpA construct is one of the most established surface display systems developed in *E. coli*[24] and has been used to display various passenger proteins with high efficiency.[15,24–25] The first nine residues of Braun's lipoprotein (Lpp) act as an anchor in the inner leaflet of the outer membrane (OM), while five transmembrane segments of OmpA are used to display the passenger protein at the C-terminal on the cell surface, in our case the SBP. SBP-displaying cells can therefore bind specifically to commercially available streptavidin coated (Sav-coated) magnetic microbeads, enabling their isolation in a massively parallel fashion.

In the context of riboswitch evolution, high ON translation rate variants can be selected through their binding to Sav-coated magnetic beads (positive selection), while low OFF translation rate variants can be selected, in principle, through their inability to bind to these beads (negative selection). In the present work, however, we decided to employ the known toxicity of Lpp-OmpA overexpression for negative selection. When chimaera expression levels are too high, they lead to cell death and major counter-selection most likely resulting from OM permeabilization and periplasmic leakage. In previous work, reduction of heterologous protein expression by reducing temperature and duration of the expression reaction, as well as induction levels was usually sufficient to mitigate such effects, provided that the passenger protein size was not too large.[15a,25b,26] In our case, we apply such measures (low temperature, short duration) to minimize cell death during positive selection rounds. Conversely, in order to drive negative selection, we extended the duration of the incubation time and maximized expression levels by increasing the temperature (Figure 1a).

To benchmark our selection system, we chose to evolve a riboswitch from the theophylline aptamer, from which riboswitches had already been developed. We thus applied our selection workflow to the fully randomized expression platform library from Lynch and Gallivan,[27] which had been previously screened using flow-cytometry (Figure 1b). In our sequence library, the theophylline aptamer is followed by a fully randomized expression platform (12 bases), which was cloned upstream of the lpp-ompA-SBP construct. A double selection cycle starts with a positive selection step, in which variants with a high ON expression level (in presence of theophylline) will be selected through binding to magnetic beads. This is followed by a negative selection step where variants with a high OFF expression level (in absence of theophylline) are counter-selected through increased cell death.

We originally placed the Lpp-OmpA-SBP chimaera expression under the control of a T7 promoter. However, even after multiple attempts to lower its expression strength, once induced our cells suffered from toxic OM destabilization. The resulting fitness cost was thus found too high to allow for positive selection. We therefore decided to place the chimaera expression under a pBAD promoter, whose expression can be better tuned, leading to a reasonable fitness cost to the induced cells, while producing detectable amounts of chimaera proteins (Figure S1).

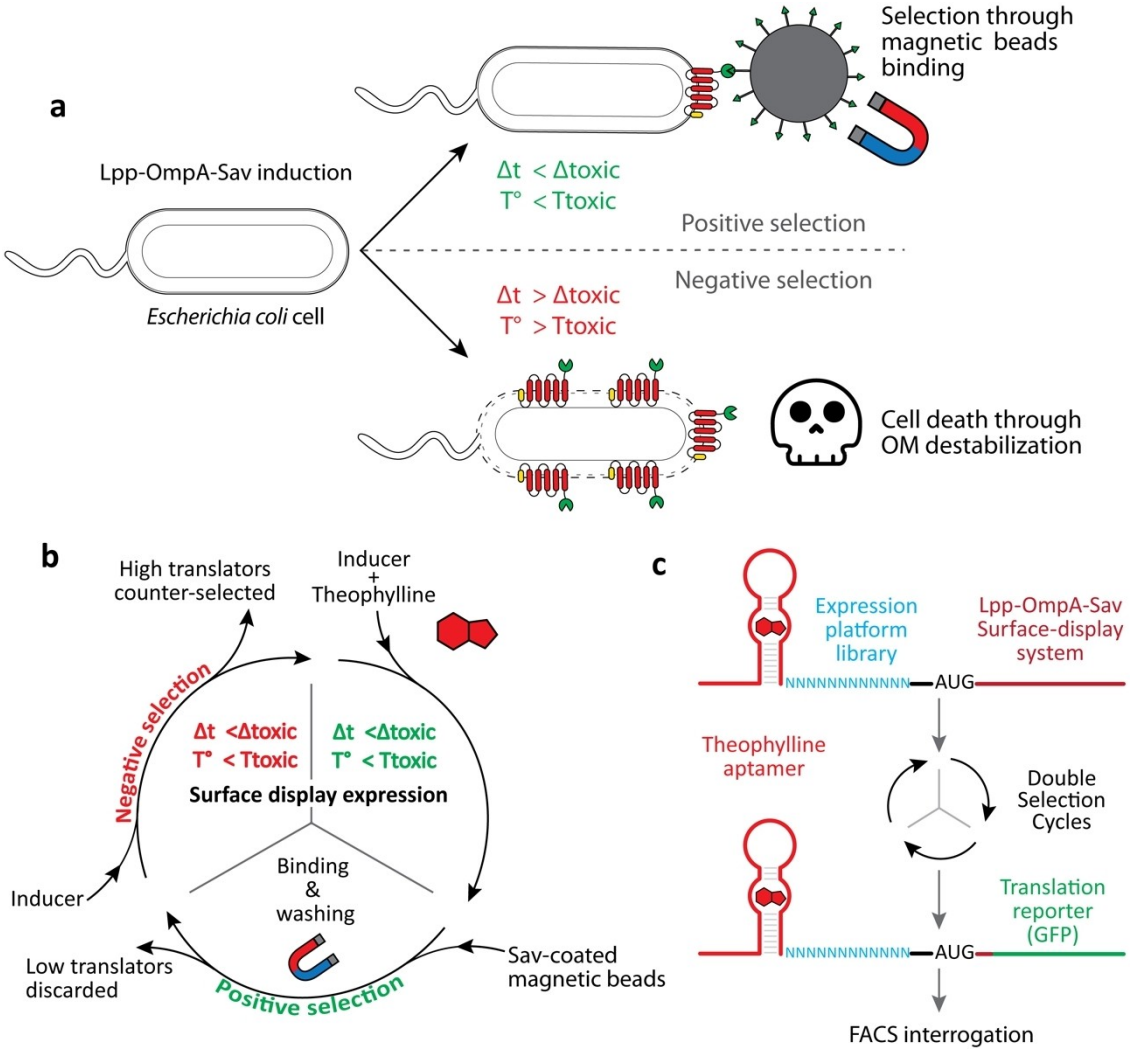

Figure 1. Double selection workflow used in this work. **(a)** Positive and negative selections after Lpp-OmpA-SBP induction. When expression is carried out at low temperature and for a limited duration, a selection through beads binding is possible. Otherwise, expression of the surface system display lead to OM permeabilization and cell death. **(b)** Double selection cycle workflow applied to an expression platform library downstream of a theophylline aptamer. In presence of theophylline, high translators are selected through beads binding but counter-selected in absence of theophylline through OM destabilization. **(c)** Before and after each double selection cycle, GFP is sub-cloned in frame downstream of the expression platform library and analysed by flow cytometry.

Fluorescence measurements of Sav-coated beads in the presence and absence of cells labelled with a dedicated chemical fluorescent cell stain (Syto 9) clearly indicated specific binding of cells expressing the chimaera protein (Figure S2). In addition, we were able to observe individual Lpp-OmpA-SBP expressing cells tightly bound to single Sav-coated beads (Video S1).

Mock positive and negative selection

Encouraged by these preliminary results, we decided to assess the specificity of binding under competitive binding conditions. To this end, cells expressing the Lpp-OmpA-SBP construct were mixed with control cells carrying either an empty plasmid or expressing LacI as a control protein and Sav-coated magnetic beads. Test and control cells were transformed with a secondary plasmid driving the constitutive expression of an orthogonal fluorescent reporter, mTurquoise and mScarlet respectively, making the colonies of each strain distinguishable from another. Microscopic observation of the mixture in the presence of a magnetic field clearly showed that the vast majority of cells bound to the beads were test cells, indicating a low level of unspecific binding of control cells (Figure 2a).

In order to develop an efficient cell sorting protocol, we subsequently performed mock selections with test and control cells. For positive selection, beads were isolated from the cell suspensions using a magnetic separation rack. The beads were plated on selective agar plates, and after colony growth we were able to identify the cells that were isolated in the separation step. As anticipated, the magnetic bead pellet was significantly enriched in SBP-displaying cells compared to the supernatant or to the suspension prior to sorting (Figure 2b). As shown in Figure 2c, cells displaying SBP on their surface were

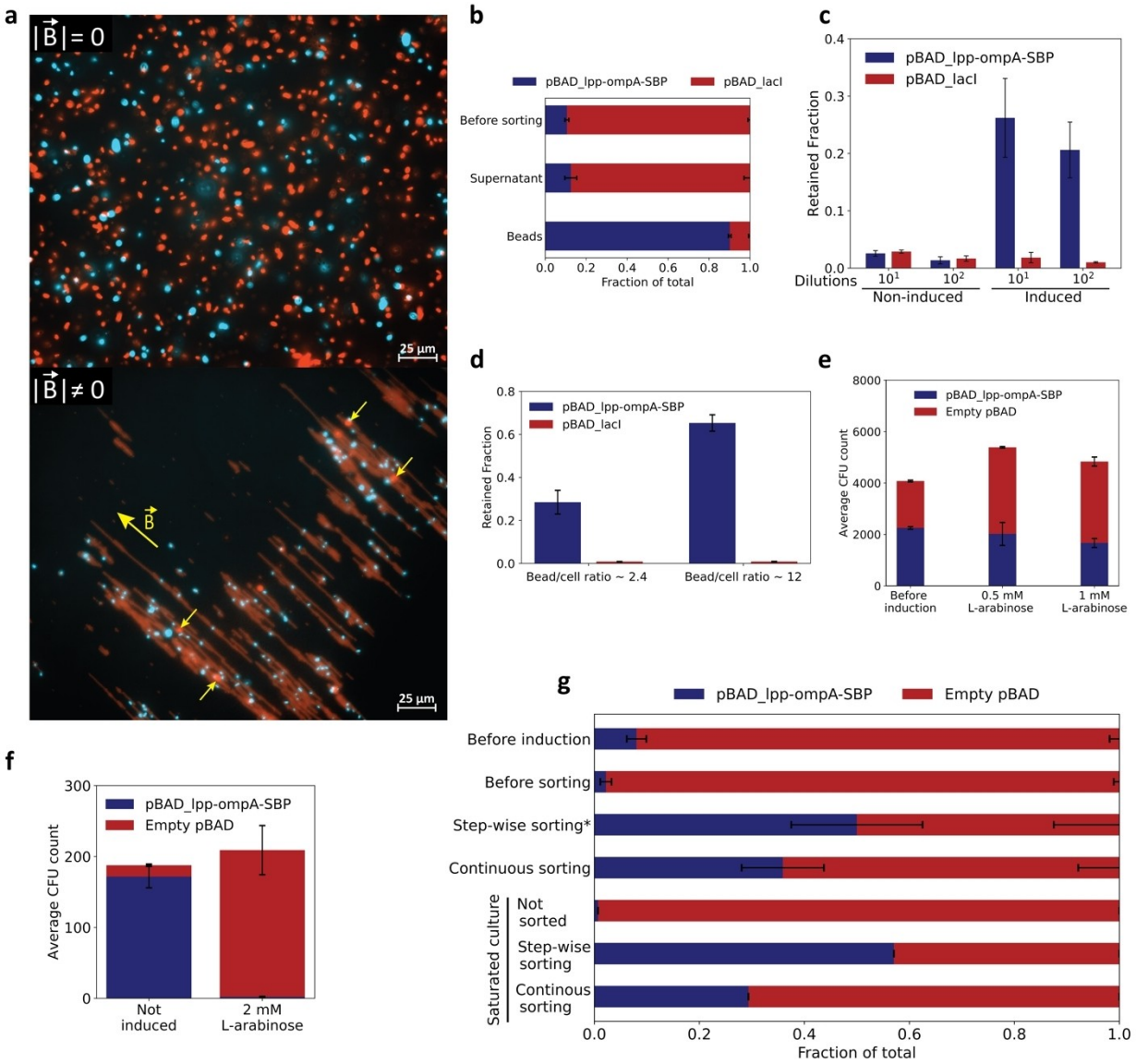

Figure 2. Mock selections through bead binding and OM destabilization. If not stated otherwise, sorting through bead binding was done with step-wise sorting. Error bars represent standard deviation obtained from 3 technical replicates. a-d: Test and control cells were cultivated separately before incubation with beads. e-g: Test and control cells were co-cultivated before incubation with beads. **(a)** Composite microscopy image of mTurquoise and mScarlet emission from test and control cells incubated with Sav-coated magnetic beads. Beads (weak autofluorescence, red signal) are aligned with the magnetic field generated by a permanent Neodymium magnet placed on top of the observation slide (bottom). Lpp-ompA-SBP chimaera expression in test cells allows a specific binding to beads (co-expressed with mTurquoise, blue signal). A few control cells, expressing LacI (co-expressed with mScarlet, red signal) are pointed out by arrows in the bottom image. **(b)** Specific binding of cells expressing Lpp-ompA-SBP chimaera. **(c)** Influence of sorting through bead binding on test and control cells proportions. Supernatant refers to cells that were still in suspension after isolation of beads with a magnet. **(d)** Influence of beads/cells ratio on retained fractions. **(e)** Mitigation of OM destabilization from Lpp-ompA-SBP-expression. Cells were incubated for only 2 h at 25 °C, 180 rpm. **(f)** Negative selection through OM destabilization. Cells were incubated for at least 16 h at 37 °C, 250 rpm. **(g)** Influence of sorting through bead binding method on test and control cells proportions. Continuous sorting: unlike step-wise sorting, magnetic pellet is not resuspended when washing but washed with a continuous stream of buffer. *: N = 2. Saturated culture: samples were grown to saturation after sorting, N = 1.

retained by Sav-coated magnetic beads considerably more compared to control cells or non-induced test cells, resulting in an enrichment of SBP expressing cells after sorting. As expected, the ratio of beads over cells influenced the final proportion of retained cells, showing that this ratio could also be used as a control parameter to tune the stringency of sorting (Figure 2d). Uncontrolled overexpression of the chimaera protein reduces fitness due to OM destabilization (see above) and would thus lead to major counter-selection. It is possible, however, to reduce counter-selection before sorting to at an acceptable level by expressing the chimaera at relatively low levels and only over a short period (Figure 2e). Even though a reduction of the fraction of test cells is always observed after chimaera expression, this is over-compensated by their enrichment after sorting (Figure 2f).

We realized that in order to improve the enrichment of test cells it is actually more relevant to minimize the number of control cells retained in the fraction than to maximize the fraction of retained test cells. In our mock selections, we decided to co-cultivate strains with a low-test cell proportion (≈10%), emulating library sorting conditions where the proportion of strong binders is also expected to be low. Under such conditions, it is mandatory to get rid of control cells (i.e., weak binders in library sorting) as effectively as possible. To this end, we compared the efficacy of two washing protocols. In "continuous sorting", the magnetic bead pellet is washed with a large volume of washing buffer, while in the superior "step-wise sorting" method the beads are repeatedly washed and resuspended in fresh washing buffer (Figure 2g). It is worth noting that the ratio between test and control cells obtained just after sorting is maintained even after a subsequent regrowth step. This indicates that once inducer is absent from the medium, test cells are not reduced in fitness compared to the control cells (cf. "saturated culture" in Figure 2g). Our mock selections helped to identify crucial parameters influencing the final enrichment such as bead-to-cell ratio, number of washing steps, binding time, temperature, buffer composition, and coating of the beads, which resulted in the optimized protocol reported in the experimental procedures. In order to perform a mock negative selection, we increased Lpp-OmpA-SBP expression levels using high induction levels and high temperature over a longer duration. The effect on the population was, as expected, massive, and test cells were almost entirely outcompeted (Figure 2f).

Magnetic selection of a theophylline riboswitch

The insights gained through our mock selections allowed us to devise an approach in which both positive and negative selection can be applied to bacterial cells. We decided to test our system on the RNA library originally utilized by Lynch and Gallivan for the selection of a theophylline riboswitch based on a theophylline aptamer[27–28] (the so-called switch 12.1 or riboswitch D, termed "reference riboswitch" in the following), which contains a randomized, 12 nt long expression platform downstream of the aptamer sequence.

We initially attempted to decouple negative and positive selection in order to assess their effects separately. Therefore, we applied several negative selection steps in the absence of theophylline, then several positive selection steps in its presence. To assess the effect of our system on the distribution of ON and OFF translation levels using FACS, we replaced the sequence downstream of the first six N-terminal residues of the lpp-ompA-SBP construct by the sequence coding for the Green Fluorescent Protein (GFP) (Figure 1c). Negative and positive selection both produced the expected effects, i.e., a decrease and increase in translation levels, respectively (Figure S3), but did not result in the emergence of proper switching behavior at the population level. Instead, after each positive or negative selection step the fluorescence of the whole population shifted towards lower or higher levels, independent of the presence of theophylline.

These results indicate that our negative selections led to bacterial populations with very tight translation inhibition showing no increase of fluorescence upon theophylline addition (riboswitches were "always OFF") (Figure S3b), whereas positive selection led to populations with leaky expression, i.e., high fluorescence levels were observed even in the absence of theophylline (riboswitches were "always ON") (Figure S3d, e). It is worth noting that after four negative and then four positive selections, a sub-population started to emerge (Figure S3c) that showed high fluorescence levels only in the presence of theophylline. These highly fluorescent phenotypes represented only a small percentage of the population and did not allow the isolation of promising individual variants, however. We therefore performed double selections on the starting library by directly executing a negative selection after each positive selection step in order to balance their impacts against each other. Already the fluorescence distribution of the initial library showed a modest switching behavior (Figure 3a) on the scale of the population, which is expected as the diversity of the expression platform library is at its maximum at this stage. The initial distribution is found to be bimodal, where the lower mode likely contains variants with strongly inhibiting switch sequences and cells with misassembled constructs. This lower mode is observed at all stages (and independent) of selection, as flawed constructs are generated during each of the GFP subcloning steps, i.e., after each of the double selection cycles. After just one round of double selection, the population started to show enhanced switching behavior, showing lower expression than the starting library in the absence of theophylline, but reaching fluorescence levels as high as the starting library in its presence (Figure 3b). This trend continued after a second round of selection (Figure 3c) making translation even more inhibited in the absence of ligand. On the other hand, fluorescence levels in its presence were almost identical as for the starting library, resulting in a more pronounced difference between ligand absence and presence.

Further double selections led to the emergence of one additional sub-population visible with or without theophylline, having an overall higher expression level and showing even more obvious switching behavior upon addition of theophylline (Figure 3d,e). The effect of each selection cycle had a considerable effect on the distribution of fluorescence levels, which hinted at a deep impact of our selection procedure on the sequence pool.

Analysis of selected riboswitch candidates

We next used FACS to sort sub-populations of interest that emerged from our double selection workflow. From the population submitted to two double selections, we sorted the cells displaying the highest levels of fluorescence in the presence of theophylline, for which we defined a sorting gate that was expected to lead to an enrichment of variants exhibiting a certain level of translation inhibition in the absence

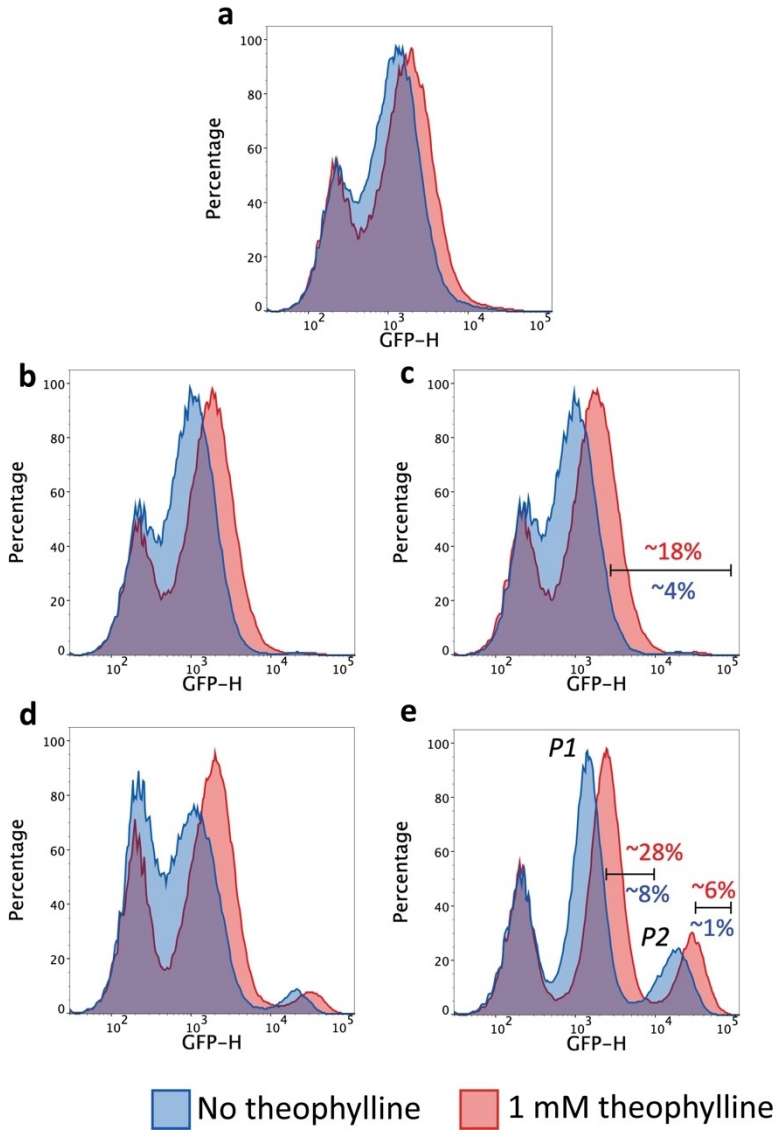

Figure 3. Double selection effects on expression levels distribution. Fluorescence intensity distribution from cells expressing GFP downstream of **(a)** starting expression platform library, **(b)** library submitted to one double selection, **(c)** library submitted to two double selections, **(d)** library submitted to three double selections, **(e)** library submitted to four double selections. The distribution of expression levels is altered after each double selection cycle and the difference between these levels in the absence and presence of the ligand becomes more pronounced (especially after two cycles, panel (c)), showing the critical effect of our double selection cycle on the expression platform library.

of theophylline (Figure 3c). Collected cells were then plated and monoclonal variants were individually screened, which showed that 85% of the variants collected in the gate exhibited a detectable switching activity. Satisfyingly, the reference riboswitch sequence originally isolated by Lynch and Gallivan was consistently found in at least 5% of the screened colonies in two independent selection experiments.

Encouraged by these results, we isolated individual variants from populations submitted to further double selections, where we also investigated the new high expression subpopulation emerging after four double selections. To this end, we positioned two sorting gates as indicated in Figure 3e, which contained 28% vs. 8% and 6% vs. 1% of the total population in the presence and absence of theophylline, respectively. The apparent ON/OFF ratio obtained from the maximum fluorescence values of the subpopulations merely represents a trend on the scale of the whole population, but not the achievable ON/OFF ratio of individual variants.

For each gate, we therefore screened 88 colonies for their switching performance and sequenced the most promising hits. Interestingly, none of these sequences was the reference riboswitch. From the gate positioned at sub-population *P2* (Figure 3e), five hits were isolated and surprisingly four out of five sequences were found identical. Although still showing switching behavior in the presence of theophylline, a variant labelled hit 4.2 carrying this sequence had an ON/OFF ratio representing only 30% of the reference riboswitch ratio. Among the cells collected from the sub-population *P1* (Figure 3e), four

hits were isolated and all were found functional riboswitches. Hit 4.1, whose sequence was found twice, showed a comparable ON/OFF ratio with the reference riboswitch and was isolated a second time in another independent sorting of sub-population *P1*.

Hit 4.1 – a functional theophylline riboswitch

We next compared the performance of the newly selected riboswitch hit 4.1 with the reference riboswitch. As shown in Figure 4a, both riboswitches showed a very similar response for theophylline concentrations below 300 μM. Hit 4.1 appeared to be slightly more responsive at concentrations lower than 200 μM, while the reference riboswitch outperformed hit 4.1 at higher concentrations. The ON/OFF ratios reported here are smaller than previously reported values, most likely because parameters such as induction levels, plasmid copy number, culture conditions and cell autofluorescence background were not adjusted optimally. Furthermore, the absolute value of ON/OFF ratio can depend on the translation reporter employed and we were primarily interested in the relative performances between hits and the reference riboswitch, not in the absolute values of ON/OFF ratios.

The better response of hit 4.1 at low theophylline concentrations might be explained by its 5′UTR secondary structure in absence of theophylline (Figure 4b). Key residues that are predicted to be required for theophylline recognition[30] are mostly solvent accessible in hit 4.1, in particular C26 and residues G31 to G34, while these residues are base-paired in the secondary structure model of the reference riboswitch.

The expression platform of hit 4.1 contains a hairpin structure that partly sequesters four residues of the Shine-Dalgarno (SD) sequence (5′-GAGG-3′), which become fully exposed upon theophylline binding to the aptamer and thus allows for translation to take place. The higher translation levels observed with the reference riboswitch at theophylline concentrations above 200 μM are likely due to a suboptimal spacing between its SD sequence and the start codon. Indeed, the SD sequence in hit 4.1 places the 5′ end of the anti-SD sequence 11 bases from the start codon whereas the optimal spacing ranges from 4 to 6 nt as in the reference riboswitch sequence.[27,31]

One of the main parameters identified in our mock selections that can be used to tune the stringency of a positive sorting step was the bead/cell ratio. Increasing this ratio will lead to more permissive sorting whereas decreasing it will focus selection on the variants exhibiting the highest translation levels. While the four double selections shown in Figure 3 were carried out with a constant ratio of 0.6, we also investigated the effect of lowering this ratio for the third and fourth selection to 0.12 and 0.06 respectively. As anticipated, this led to higher fluorescence levels in the presence of theophylline (Figure S4). However, fluorescence levels were also higher in the absence of theophylline, showing that leak translation from the switch in the OFF state had increased. Quite interestingly, as in the selections performed with a constant bead/cell ratio, a high fluorescence subpopulation emerged. After the fourth selection, gating of these sub-populations through flow cytometry led to the isolation of individual variants showing a large proportion of functional switches with very high absolute fluorescence levels (among which hit 4.2 was found again), but none of them presented an ON/OFF ratio as good as the reference riboswitch.

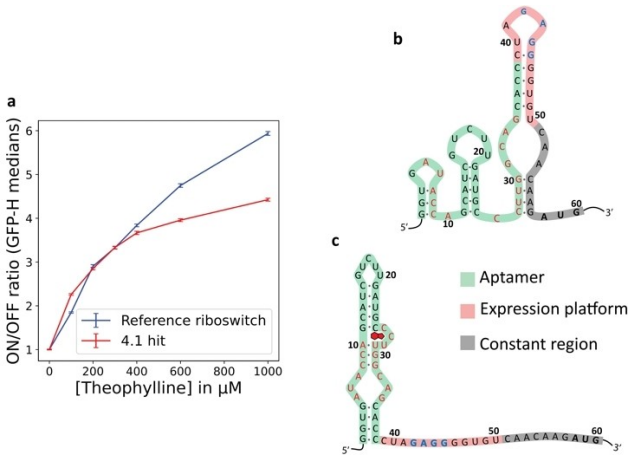

Figure 4. Characterization of hit 4.1. **(a)** Response curve of hit 4.1 and reference riboswitch. ON/OFF ratios were calculated with averages over GFP–H medians obtained from 3 technical replicates through flow cytometry. Prediction of hit 4.1 5′UTR secondary structure in absence **(b)** or presence **(c)** of theophylline. Residues in red are required for theophylline recognition. Residues in blue represent the putative Shine-Dalgarno sequence. 5′UTR prediction structure in absence of theophylline was obtained from NUPACK web application[29] whereas aptamer structure in its presence was depicted as in previous literature.[27–28,30]

Discussion

The main advantage of the double selection workflow described here is the possibility to apply a coarse – but massively parallel – pre-selection on a library of riboswitches that allows enrichment of the population with promising variants before FAC sorting. Indeed, most variants of a randomized sequence library are expected to perform poorly – i.e., in the case of the present expression platform library a very low ON/OFF ratio is expected initially. When screening a library only through FACS, the gated populations will contain only few promising hits, which requires screening a large number of individual colonies after sorting. Our workflow allows the removal of most of the poorly performing variants from the sequence pool before submission to FACS in a facile and highly parallel manner. As our selection system does not include a "gating step" such as in FACS (all cells are either bound to beads, or washed away) the time required to perform a double selection on a given library is not linearly dependent on its size or on the number of variants to sort. Furthermore, the workload for selection is relatively low (most of the time is required for cell culture and gene expression) and a full double selection can be completed in a day (negative selection by cell culture is carried out overnight). In our workflow, flow cytometry is only used after the population had already been heavily enriched in

good performers, making FACS-based and colony screening comparatively brief. In fact, we never had to screen a large number of individual colonies in order to find a relevant hit. For instance, the number of plated cells after sub-population gating never exceeded 400 colonies and all mentioned hits were found at least once in each multiwell plate used for screening. As each plate allows to interrogate 88 individually picked colonies, screening this number of variants for each FACS gating would have been already sufficient to discover all hits. This represents a considerably reduced individual colony screening workload compared to what is usually required for high-throughput screening, and is easily achievable without the help of automated techniques such as a robotic colony picker. The percentage of colonies displaying a positive response upon addition of theophylline was extremely high, ranging between 60% and 90% for different screenings, which indicates a strong enrichment of the library by the bead-based pre-selection step.

Our double selection results in a fluorescence level distribution which is suitable for gating by FACS. In our case, the cell fraction displaying the higher fluorescence levels after two selection rounds (Figure 3c) contained only few cells in the absence of theophylline, but a much larger fraction upon its addition. Such a distribution ensures that the variants in the gating window indeed display switching behavior.

We were also able to consistently observe sequence redundancy among our best selection hits. Well-performing sequences were always found multiple times within the same gating window, suggesting a loss of sequence diversity and convergence throughout double selections and FACS.

Remarkably, though, the reference riboswitch was found after only two double selections, while the 4.1 hit was not found at all, whereas after four double selections the latter was found multiple times and the reference riboswitch was not detected. This indicates that the reference riboswitch was counter-selected against and lost during the third and fourth double selection rounds, or FACS.

Our parallel workflow helps to thoroughly screen the phenotypes generated by the sequences of a given library. In this work, we used our knowledge of a reference riboswitch to test the effectiveness of our method. The sequence convergence we observed suggests that the re-discovered reference riboswitch sequence is already the "optimal" sequence with the highest ON/OFF ratio in *E. coli* within the library. However, it is worth noting that after transformation, we estimated our in vivo library size to only cover 70% of the whole sequence space (1.68×10^7 possible combinations), so there may be other interesting variants that were not present in our in vivo library.

Our system can be theoretically applied to the selection of different types of riboswitches, translational or transcriptional, ON or OFF switches, the latter being selectable with our system by supplementing ligand during negative selection steps and omitting it in positive steps. As mentioned above, the workload required to perform a selection with our system is not linearly linked to the size of the library to be screened. This potentially enables the screening of very large randomized expression platform libraries without additional workload (if an aptamer for a specific ligand had already been identified), or even selecting expression platform and aptamer domain at the same time (if the library/library size allows it). Such a way of evolving switches would help to select for aptamers that can function as conformational switches, which is in contrast to selection through conventional SELEX.

For other specific selection tasks, several challenges will have to be addressed. For instance, one limitation of our system is that above a certain ON translation level, library variants might not be selectable through their binding to beads any more. For instance, translation activity could be so high that the deleterious effects due to Lpp-ompA expression will diminish the fitness conferred by the affinity to the beads during positive selection. In such a case, the positive selection conditions would have to be tuned carefully to reduce Lpp-ompA expression toxicity even further. Another challenge that could arise during the selection of high-level translators is that the dynamic range of the affinity of the cells for binding to the beads is not large enough. Once the expression level reaches a certain threshold, all variants will have achieved a maximum level of SBP surface display, resulting in saturated binding to the beads. Thus, higher translation levels would not lead to an enrichment but rather to counter-selection that favors variants displaying just enough SBP to ensure a maximum affinity for beads. One way to extend the dynamic range towards higher translation levels would be to make binding to beads even more stringent, for example, by lowering the binding time, increasing the amount of blocking agents or use beads with a different surface coating.

A major challenge for the application of our workflow is a problem inherent to the evolution of molecular switches in general: for a good switch, two criteria – low OFF and high ON activity – must be simultaneously fulfilled, so any change in stringency in one selection step (positive or negative) presumably has to be met by a corresponding change in the opposite selection step. A loss of balance between positive and negative selection will likely lead to the selection of poor switches, as successful variants will only meet one of the two criteria, not both. For instance, by lowering the bead/cell ratio (Figure S4), the population was submitted to a very stringent positive selection and, consequently, the variants isolated from it displayed very high ON rates but also high OFF rates, resulting in sub-optimal switching behavior.

In such a case, negative selection has to be tuned accordingly. Also, if stringency is extremely high, the most probable outcome will be that in order to pass rigorous sorting, successful library variants will not exhibit any switching behavior, but will display constitutive OFF translation repression or constitutive ON translation activation. In other words, in order to employ our selection system most efficiently, one has to consider which ON/OFF ratios can be realistically achieved. On the other hand, if selection steps are too permissive, the selection pressure will not be sufficient to remove library variants displaying low ON/OFF ratios (which by far are the most abundant in a starting library), and the sequence pool will not be shaped efficiently in the desired fashion. Determining the optimal trade-off for the selection steps is an empirical

process, and our system enables this by allowing flexible tuning of the selection stringencies and observation of their effects.

Conclusion

We have developed a selection workflow using the Lpp-ompA-SBP surface-display system that allows us to select or counter-select a given cell population with the help of magnetic beads. By adjusting different critical parameters, we were able to fine tune the selection process. Our system is particularly useful for conducting a large-scale selection on populations, as it does not rely on individual gating steps and the library size does not significantly impact the time required for selection. This means that sequence pools can be directed towards a particular goal, which can help streamline the subsequent screening process.

We tested our system by evolving a riboswitch, for which we used a known library for a proof of principle. Our results show that our system is effective at finding functional riboswitches, including one with a similar ON/OFF ratio than the reference at low theophylline concentrations.

Experimental Section

All secondary structures of mRNA 5'UTRs in absence of theophylline were obtained from the NUPACK web application.[29] For 5'UTRs in presence of theophylline, only the expression platform secondary structure was obtained from NUPACK whereas the aptamer structure upon theophylline binding was depicted as in previous literature.[27–28,30,32]

Cloning: Enzymes and buffers used for cloning were purchased from New England Biolabs (NEB) and used following standard protocols, DNA primers were purchased from IDT. All PCR purifications were performed with the Monarch Clean-up PCR kit (NEB), plasmid isolations from bacterial cell culture with the QiaPrep Spin Miniprep kit (QIAGEN). All bacterial cell cultures were performed at 37 °C, 250 rpm in LB medium supplemented with carbenicillin (100 μg/mL) unless stated otherwise. Sanger-sequencing was performed by Eurofins over isolated plasmids. All TOP10 cells used for transformation were from Invitrogen (One Shot™ TOP10 Electrocomp™ *E. coli*).

Mock selections strains cloning: A pET28b (+) vector carrying an insert encoding the Lpp signal peptide sequence, the 9 first N-terminal Lpp residues, the five first N-terminal β-barrels of OmpA followed by a linker sequence (GGGGS) and the SBP sequence was used as template for a PCR reaction using primers flanking the insert. A linear backbone was amplified using a pBAD vector carrying a lacI insert as template. Both pairs of primers were carrying a 20 bp long overhang complementary to one end of the other PCR product in order to create 40 bp long overlaps between the two linear products. The construct was circularized by Gibson assembly, then transformed into chemo-competent Turbo NEB *E. coli* cells by thermal shock (incubated during 1 h on ice, 42 sec at 45 °C then 5 min on ice) and after 1.5 h of recovery in SOC medium at 37 °C 250 rpm, cells were plated on selective LB agar plates. Colonies were submitted to colony PCR and subsequent linear products purified and verified by Sanger sequencing. A correctly assembled plasmid was then isolated from cell cultures and co-transformed with a pSB4 K5 vector carrying an mTurquoise sequence, in TOP10 background cells. Transformation was done at 1500 V and cells were recovered during 2 h in SOC medium at 37 °C, 250 rpm, then plated on double selection plates containing LB-agar supplemented with carbenicillin and kanamycin (50 μg/mL). Likewise, a pBAD vector carrying either no insert or a sequence coding for LacI was co-transformed with a pSB4 K5 vector carrying an mScarlet sequence in TOP10 background cells.

Expression platform library cloning: A linear construct was obtained by PCR using a pBAD vector carrying the lpp-ompA-SBP ORF as a template with a forward primer binding to the 5' end of the lpp sequence with an overhang carrying a 7 base constant sequence (CAACAAG) upstream of the start codon, a 12-base randomized expression platform (machine-mixed) and the 13 last bases of the theophylline aptamer and a reverse primer binding to the pBAD promoter sequence with an overhang carrying the 25 first bases of the theophylline aptamer. The PCR product was then submitted to phosphorylation (PNK), overnight T4 ligation and DpnI digestion prior to purification and transformation into TOP10 background cells at 2000 V. Cells were recovered in 10 mL SOC medium at 37 °C, 250 rpm, for 1 h before carbenicillin addition. Library size in vivo was estimated by plating different cells culture dilutions 1 h after transformation on selective LB agar plates. Initial library in vivo was obtained by pooling 3 different transformation batches whose library size were estimated to, 3.5×10^6, 1.2×10^7, and 9.5×10^5. The location of the randomized region was verified by Sanger-sequencing of colony PCR product of individual colonies.

GFP subcloning: Plasmid libraries (containing either the starting library or after different selection steps) were purified from cell cultures and used as template for a PCR reaction with a reverse primer binding to a region spanning the constant sequence downstream of the library (CAACAAG) and 18 nt at the 5' end of the lpp sequence and a forward primer binding to 25 bp of the pBAD backbone downstream of the lpp-ompA-SBP ORF. A second PCR product was obtained using a pSB4 K5 plasmid carrying a *gfp* sequence as a template and primers binding to 5' and 3' end of the gfp ORF. Both pairs of primers carried a 20 bp long overhang complementary to one end of the other PCR product in order to create 40 bp long overlaps between the two linear products. The construct was circularized by Gibson assembly and subsequently submitted to DpnI digestion, purified and transformed in TOP10 background cells as described above. To obtain the reference riboswitch from Lynch and Gallivan, the latter construct was used as template for a PCR reaction with a reverse primer binding to the theophylline aptamer region and a forward primer binding to 30 bp downstream of randomized region and carrying an overhang of 12 bp containing the original 12.1 hit sequence found by Lynch and Gallivan (5'-CTGCTAAGGTAA-3'). The PCR product was submitted then to phosphorylation (PNK), overnight T4 ligation and DpnI digestion prior to purification, transformation into TOP10 background cells, and plating on selective LB agar plates. Proper assembly of the construct was verified by sequencing colony PCR products from transformation plate.

Selections: Theophylline (anhydrous) was bought from Sigma-Aldrich and dissolved into 0.1 M NaOH. Streptavidin-coated super-paramagnetic beads (Dynabeads) with hydrophilic (C1) and hydrophobic (T1) coating were bought from Invitrogen. Bead/cell ratios were calculated thanks to beads density specified in Invitrogen product details and to the $OD600_{nm}$ of bacterial cell cultures. Before binding, bacterial cells were harvested through centrifugation (4 °C, x 3000 G) then resuspended in PBS (Gibco™, pH = 7.4) supplemented with 0.2% w/v BSA (VWR Chemicals) and beads were washed three time prior to binding with the same buffer, using a neodymium external magnet (Supermagnete, Germany).

Mock selections: For colony counting, petri dishes were scanned with a Typhoon FLA 9500 laser scanner (GE Healthcare) using the

appropriate channels to detect mTurquoise and mScarlet emission and colonies were automatically counted using image processing tools (Fiji). Cells carrying a pBAD_lacI with a pSB4 K5_mScarlet and cells carrying a pBAD_lpp-ompA-SBP with a pSB4 K5_mTurquoise were cultivated separately in liquid LB medium supplemented with carbenicillin and kanamycin (50 μg/mL). When the OD reached 0.6, cultures were induced or not with 1 mM L-arabinose and further incubated separately at 16 °C, 180 rpm for 16 h. The two cell suspensions were mixed together into various proportions, bead suspensions were added in order to reach the desired bead/cell ratio, and were then further incubated for 1 h at room temperature under gentle shaking. Beads were then isolated with a magnetic particle concentrator Dynal MPC™-S (Invitrogen) and were resuspended into fresh sterile PBS 0.2% BSA. This step was repeated 6 times after which the suspension was supplemented with 50 μM biotin and incubated for 1 h at room temperature under gentle shaking following which cells were diluted and plated on selective agar plates. Unsorted samples consisted of cell suspensions (strains mixed in the same proportion than in the sorted samples) submitted to the same dilutions than the sorted samples but no beads were added nor sorting performed. The average CFU was obtained over three technical replicates for each sample, and the retained fraction was calculated by dividing the CFU obtained for a given sorted sample and a given strain by the CFU obtained from the corresponding unsorted sample. Error bars for the retained fraction were calculated using error propagation from the standard deviation. Cells carrying an empty pBAD with a pSB4 K5_mScarlet and cells carrying a pBAD_lpp-ompA-SBP with a pSB4 K5_mTurquoise were inoculated with an initial proportion of 90% and 10% respectively and co-cultivated. When the OD reached 0.6, the co-culture was induced at 1 mM arabinose and incubated for 2 h at 25 °C 180 rpm, after which cells were sorted using the same procedure explained earlier but incubation of beads and cells together was done for 15 min on ice with gentle shaking. Cell suspensions were sampled at different stages, before induction and just before sorting, submitted to the same dilutions as the sorted samples, and were subsequently plated. Colonies plated from sorted samples were usually not numerous enough to estimate accurately the ratio between the two different strains, so after sorting, bead pellets were resuspended in selective LB medium supplemented with 50 μM biotin, incubated overnight under standard culture conditions, and then plated on selective LB agar plates with the relevant dilution. Mock negative selection through fitness cost was achieved by co-cultivating cells carrying an empty pBAD with a pSB4 K5_mScarlet and cells carrying a pBAD_lpp-ompA-SBP with a pSB4 K5_mTurquoise with an initial proportion of 5% and 95% respectively, with or without 2 mM L-arabinose for 15 h then cultures were plated.

Alternated selections: Four negative selections were performed by cultivating cell cultures carrying the expression platform library up to OD saturation in the presence of 1 mM L-arabinose, and the saturated culture was used to inoculate the next culture. Positive selections were performed by applying the same protocol described for mock positive selections with co-cultures, except that 1 mM theophylline was supplemented at the moment of induction and that cells were washed 3 times in PBS 0.2% BSA before incubation with beads in order to remove any biotin in the supernatant.

Double selections: A double selection cycle was established by first performing a positive selection step (as described earlier, in presence of 1 mM theophylline). After sorting, bead pellets were resuspended in selective LB medium supplemented with 50 μM biotin and incubated for 1 h at standard condition for bacterial culture. Then 1 mM L-arabinose was added and samples were incubated overnight in order to perform a negative selection step. Two selection protocols were carried out, one with a constant bead/cell ratio of 0.6 in the positive selection step, the other with decreasing ratios of 0.6, 0.6, 0.12 and 0.06 for the first, second, third and fourth selection, respectively.

Flow cytometry: FACS buffer used for washing and bacterial cell/beads resuspension was ice cold, sterile filtered PBS. When assessing beads-cell interaction by FACS, cells were stained with 2.5 μM Syto9 stain (ThermoFischer Scientific) for 45 min on ice, then washed two times with FACS buffer. Dynabeads (diluted 50 times from stock solution) were washed three times in FACS buffer, incubated with stained cells for 1 h at 16 °C, 150 rpm then directly submitted to FACS interrogation. When interrogating bacterial cell cultures carrying plasmid libraries, cells were washed 2 times and then diluted 100 times into FACS buffer before being sampled. Monoclonal bacterial cell cultures were directly diluted 100x into the FACS buffer. Flow cytometry data was acquired with BD FACS Melody Cell Sorter and data was analyzed with FlowJo version 10.8.1. GFP was excited using a 488 nm laser and emission was measured with a 527/35 bandpass filter. The bacterial cell population was gated on an FSC/SSC scatter plot (height) and 10^5 events were recorded for analysis. For each sorting step, 5000 cells were sorted and collected into PBS, and one tenth of the final volume was plated on selective LB agar plates.

Individual variant screening: Individual colonies were picked and precultures were cultivated on 96-well microtiter plates. After overnight incubation, each preculture was diluted 100 times into 96-well plates (IBIDI) filled with selective LB medium supplemented with 1 mM L-Arabinose in the presence or absence of 1 mM theophylline and subsequently cultivated overnight. Fluorescence and optical density were measured with a CLARIOstar microplate reader (BMG Labtech) and variants displaying the most promising ON/OFF ratios of GFP fluorescence were identified. Promising monoclonal variants were sequenced, cultivated into individual tubes containing LB medium supplemented with 1 mM L-Arabinose and different theophylline concentrations and interrogated by cytometry.

In all screening experiments, a strain carrying the same construct as the screened variants but with the sequence of the theophylline riboswitch discovered by Lynch and Gallivan in the expression platform library location was used as a control.

Microscopy: Microscopy images and videos were acquired with a Nikon Ti-2E microscope using a 20× plan apochromat oil objective (NA 1.40), 1.5× magnification, a SOLA SM II LED light source, an Andor NEO 5.5 camera and NIS elements software. Videos monitoring cells and bead binding were acquired in a microfluidic chamber designed in our lab. Cells carrying a pBAD_lacI with a pSB4 K5_mScarlet and cells carrying a pBAD_lpp-ompA-SBP with a pSB4 K5_mTurquoise were cultivated separately in liquid LB medium supplemented with carbenicillin and kanamycin (50 μg/mL). When their OD reached 0.6, the cultures were induced with 1 mM L-arabinose and further incubated for 2 h at 25 °C, 180 rpm. The two strains were resuspended into PBS 0.2% BSA, mixed at equal volume, incubated with Sav-coated beads for 30 min and then transferred onto observation slides with an external magnet placed on top.

Characterization of protein expression by PAGE: For each gel track, 200 μL of saturated *E. coli* culture were resuspended in 20 μL of Laemmli sample buffer (Sigma), incubated 10 min at 95 °C then loaded on a 12.5% SDS-PAGE gel. Gel was run at 250 V for 45 min, stained with Roti-Blue quick solution (Carl Roth) and imaged with a Quantum CX5 gel documentation imaging system (Vilber).

Supporting Information

Figures S1–S4, Tables S1-S3.

Acknowledgements

This project has received funding from the European Commission's Horizon 2020 research and innovation program under the Marie Skłodowska-Curie grant agreement no. 813786 (EVOdrops). Open Access funding enabled and organized by Projekt DEAL.

Conflict of Interests

The authors declare no conflict of interest.

Data Availability Statement

The data that support the findings of this study are openly available in Zenodo at https://doi.org/10.5281/zenodo.7716555, reference number 7716555.

Keywords: directed evolution · high-throughput screening · molecular switches · RNA · synthetic biology

[1] G. P. Smith, *Science* **1985**, *228*, 1315–1317.
[2] a) A. Charbit, J. C. Boulain, A. Ryter, M. Hofnung, *EMBO J.* **1986**, *5*, 3029–3037; b) R. Freudl, S. MacIntyre, M. Degen, U. Henning, *J. Mol. Biol.* **1986**, *188*, 491–494.
[3] G. Pozzi, M. Contorni, M. R. Oggioni, R. Manganelli, M. Tommasino, F. Cavalieri, V. A. Fischetti, *Infect. Immun.* **1992**, *60*, 1902–1907.
[4] E. T. Boder, K. D. Wittrup, *Nat. Biotechnol.* **1997**, *15*, 553–557.
[5] M. Ho, S. Nagata, I. Pastan, *Proc. Natl. Acad. Sci. USA* **2006**, *103*, 9637–9642.
[6] a) J. Schuurmann, P. Quehl, G. Festel, J. Jose, *Appl. Microbiol. Biotechnol.* **2014**, *98*, 8031–8046; b) M. L. Pham, M. Polakovic, *Int. J. Biol. Macromol.* **2020**, *165*, 835–841; c) A. Bielen, R. Teparić, D. Vujaklija, V. Mrša, *Food Technol. Biotechnol.* **2014**, *52*, 16–34.
[7] M. L. Wu, C. Y. Tsai, T. H. Chen, *FEMS Microbiol. Lett.* **2006**, *256*, 119–125.
[8] C. Yang, R. Freudl, C. Qiao, A. Mulchandani, *Appl. Environ. Microbiol.* **2010**, *76*, 434–440.
[9] S. Shibasaki, in *Yeast Cell Surface Engineering: Biological Mechanisms and Practical Applications* (Ed.: M. Ueda), **2019**, pp. 149–158.
[10] a) L. Han, Y. Zhao, S. Cui, B. Liang, *Appl. Biochem. Biotechnol.* **2018**, *185*, 396–418; b) S. Zhao, G. Yang, X. Xie, G. Yan, F. Wang, W. Chen, L. Ma, *Biomol. Eng.* **2022**, *12*.
[11] M. Park, *Sensors* **2020**, *20*, 2775.
[12] a) P. E. Saw, E. W. Song, *Protein Cell* **2019**, *10*, 787–807; b) J. Bowen, J. Schneible, K. Bacon, C. Labar, S. Menegatti, B. M. Rao, *Int. J. Mol. Sci.* **2021**, *22*, 1–20; c) A. T. Tucker, S. P. Leonard, C. D. DuBois, G. A. Knauf, A. L. Cunningham, C. O. Wilke, M. S. Trent, B. W. Davies, *Cell* **2018**, *172*, 618–628e613.
[13] V. Salema, L. A. Fernandez, *Microb. Biotechnol.* **2017**, *10*, 1468–1484.
[14] Y. S. Kim, H. C. Jung, J. G. Pan, *Appl. Environ. Microbiol.* **2000**, *66*, 788–793.
[15] a) S. Nicchi, M. Giuliani, F. Giusti, L. Pancotto, D. Maione, I. Delany, C. L. Galeotti, C. Brettoni, *Microb. Cell Fact.* **2021**, *20*, 33; b) E. van Bloois, R. T. Winter, H. Kolmar, M. W. Fraaije, *Trends Biotechnol.* **2011**, *29*, 79–86.
[16] a) A. S. Mironov, I. Gusarov, R. Rafikov, L. E. Lopez, K. Shatalin, R. A. Kreneva, D. A. Perumov, E. Nudler, *Cell* **2002**, *111*, 747–756; b) A. Nahvi, N. Sudarsan, M. S. Ebert, X. Zou, K. L. Brown, R. R. Breaker, *Chem. Biol.* **2002**, *9*, 1043; c) W. Winkler, A. Nahvi, R. R. Breaker, *Nature* **2002**, *419*, 952–956.
[17] J. E. Barrick, R. R. Breaker, *Genome Biol.* **2007**, *8*, R239.
[18] M. Etzel, M. Morl, *Biochemistry* **2017**, *56*, 1181–1198.
[19] a) A. Boussebayle, D. Torka, S. Ollivaud, J. Braun, C. Bofill-Bosch, M. Dombrowski, F. Groher, K. Hamacher, B. Suess, *Nucleic Acids Res.* **2019**, *47*, 4883–4895; b) J. O. L. Andreasson, M. R. Gotrik, M. J. Wu, H. K. Wayment-Steele, W. Kladwang, F. Portela, R. Wellington-Oguri, P. Eterna, R. Das, W. J. Greenleaf, *Proc. Natl. Acad. Sci. USA* **2022**, *119*, e2112979119.
[20] N. Muranaka, V. Sharma, Y. Nomura, Y. Yokobayashi, *Nucleic Acids Res.* **2009**, *37*, e39.
[21] S. Topp, J. P. Gallivan, *ChemBioChem* **2008**, *9*, 210–213.
[22] T. Peschke, K. S. Rabe, C. M. Niemeyer, *Angew. Chem. Int. Ed. Engl.* **2017**, *56*, 2183–2186.
[23] A. D. Keefe, D. S. Wilson, B. Seelig, J. W. Szostak, *Protein Expression Purif.* **2001**, *23*, 440–446.
[24] J. A. Francisco, C. F. Earhart, G. Georgiou, *Proc. Natl. Acad. Sci. USA* **1992**, *89*, 2713–2717.
[25] a) R. D. Richins, I. Kaneva, A. Mulchandani, W. Chen, *Nat. Biotechnol.* **1997**, *15*, 984–987; b) T. Heinisch, F. Schwizer, B. Garabedian, E. Csibra, M. Jeschek, J. Vallapurackal, V. B. Pinheiro, P. Marliere, S. Panke, T. R. Ward, *Chem. Sci.* **2018**, *9*, 5383–5388; c) C. Hui, Y. Guo, W. Zhang, C. Gao, X. Yang, Y. Chen, L. Li, X. Huang, *Sci. Rep.* **2018**, *8*, 5685.
[26] a) H. Shi, W. Wen Su, *Enzyme Microb. Technol.* **2001**, *28*, 25–34; b) S. Gallus, E. Mittmann, K. S. Rabe, *ChemBioChem* **2022**, *23*, e202100472.
[27] S. A. Lynch, J. P. Gallivan, *Nucleic Acids Res.* **2009**, *37*, 184–192.
[28] S. Topp, C. M. Reynoso, J. C. Seeliger, I. S. Goldlust, S. K. Desai, D. Murat, A. Shen, A. W. Puri, A. Komeili, C. R. Bertozzi, J. R. Scott, J. P. Gallivan, *Appl. Environ. Microbiol.* **2010**, *76*, 7881–7884.
[29] a) J. N. Zadeh, C. D. Steenberg, J. S. Bois, B. R. Wolfe, M. B. Pierce, A. R. Khan, R. M. Dirks, N. A. Pierce, *J. Comput. Chem.* **2011**, *32*, 170–173; b) M. E. Fornace, J. Huang, C. T. Newman, N. J. Porubsky, M. B. Pierce, N. A. Pierce, **2022**.
[30] A. Wrist, W. Sun, R. M. Summers, *ACS Synth. Biol.* **2020**, *9*, 682–697.
[31] H. Chen, M. Bjerknes, R. Kumar, E. Jay, *Nucleic Acids Res.* **1994**, *22*, 4953–4957.
[32] R. D. Jenison, S. C. Gill, A. Pardi, B. Polisky, *Science* **1994**, *263*, 1425–1429.

Manuscript received: March 16, 2023
Accepted manuscript online: April 20, 2023
Version of record online: May 11, 2023